Chapter 6

Sensors, actuators, and interfaces

Contents

This chapter surveys some of the most common components that attach to SBCs to form useful cyber-physical (aka electro-mechanical) systems. These components generally come in three broad categories: **sensors**, **actuators**, and **user interfaces**. Though not exhaustive, we will discuss many representative examples of components in each of these categories in turn in this chapter; a brief survey of how such components may be put together to make larger systems is deferred to §17. We begin with a brief discussion of how to get power and signal on and off of the moving parts of the system.

6.1 Brushes & commutators vs rotary transformers

It is often necessary to transfer power and/or signals on or off of rotating shafts that coordinate the motion of wheels, linkages, and other moving parts. Applications in which this need arises, among many, include:

- low-cost BDC *motors* (see §6.8),
- analog devices, called *resolvers*, used to measure shaft rotation (see §6.2.3),
- *robot arms* capable of large ranges of motion (see Figure 6.3c and §17.9.3),
- rotating sets of LEDs leveraging the *persistance of vision* (PoV) effect to make images (see §6.14.4), etc.

There are four main methods of accomplishing such transfers to rotating frames:

(a) brushes and commutators (Figure 6.1, discussed further below),
(b) rotary transformers (Figure 6.2, also discussed further below),
(c) local COTS wireless communication protocols (§3.4) like bluetooth[1] (§3.4.2), and
(d) flexible wires with careful cable routing[2], in applications for which the total rotation is limited (Figure 6.3).

The cheapest method is to use stationary spring-loaded carbon or copper **brushes**, mounted to rub against (and, to make reliable electrical contact with) rotating conductive rings called **commutators** (see Figure 6.1). This approach can efficiently pass both low-bandwidth logical signals, as well as both alternating current (AC) and direct current (DC) power, from the stationary frame to the rotating frame, but often introduces significant electrical noise, motivating the use of some low-pass filtering (see §9 and §10) to remove. Commutators can either be the **continuous-ring** type, which provide continuous electrical contact as the shaft turns, or the **split-ring** type, which mechanically break the electrical connection when the shaft turns past a certain angle, and then reform the electrical connection, with the opposite polarity, as the shaft continues to turn further. Note that the clever use of split-ring commutators forms an essential component of the operation of brushed DC (BDC) motors, discussed in §6.8. Either way (using continuous-ring or split-ring commutation), due to mechanical wear, the brushes will eventually wear out. Most small BDC motors are designed be disposed of when the brushes wear out; in some older/larger BDC motors, the brushes may be replaceable by the user. Most newer large motors are brushless (see §6.9), which are more efficient and require less maintenance.

A more durable method for transferring power and signals to and from rotating frames is to use **rotary transformers**. With this approach, magnetically-coupled electromagnets are placed near to each other, one on the rotating shaft, and the other on its stationary housing. One of these electromagnets is driven by an AC input (typically oscillating at a frequency ω_e that is fast wrt the shaft rotation); by **magnetic induction**, a concomitant AC current is picked up by the other electromagnet. Typical configurations are illustrated in Figure 6.2. This approach is more durable than using brushes and commutators, but can only handle AC signals and, depending on the strength of the magnetic coupling in the design, typically suffers 30% or higher power loss. This power loss is turned directly into waste heat, which means that rotary transformers are generally not well suited for power transfer in high-current applications.

[1] COTS bluetooth solutions are low latency, low power, and inexpensive, and are often preferred in high-bandwidth applications.
[2] Note that such wires must be routed very carefully, in order to not tug or foul during operation, or to fatigue too quickly.

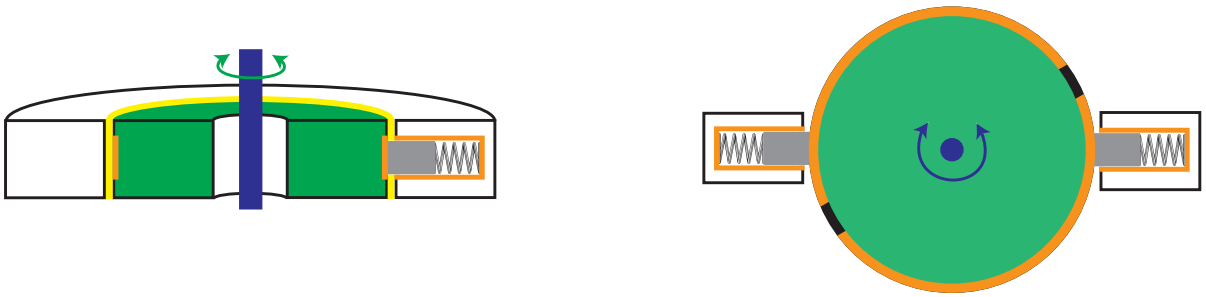

Figure 6.1: Brush & commutator systems for transferring both DC and AC power and signals between rotating (green) and non-rotating parts. (a) Side (cut-away) view of a **continuous-ring commutator**; a spring is usually used to keep the (relatively soft) carbon or copper brush (gray), which is stationary, in constant contact with the ring (orange) mounted to the rotating component (green) attached to shaft (blue). (b) Top view of **split-ring commutator** for coordinated excitation of the rotating electromagnets of a BDC motor (see §6.8); note that the width of the nonconductive split (black) must be larger than the width of the brush in the azimuthal direction, so that a short between the two inputs (left and right) can not occur. Images are cartoon representations only; for notational clarity, the housings and bearings that keep the parts aligned and spinning freely are not shown.

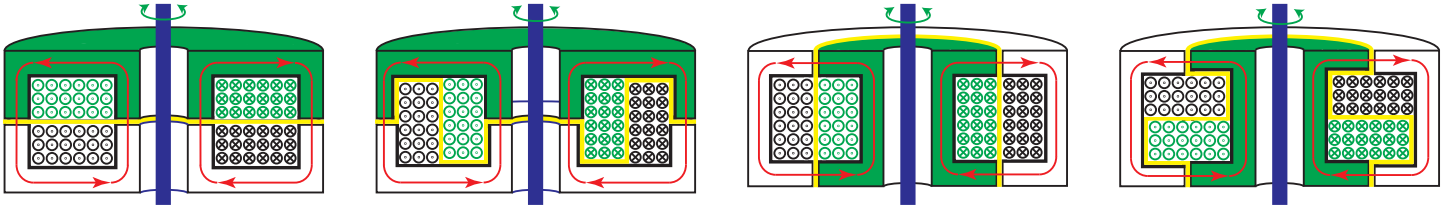

Figure 6.2: Four different configurations of **rotary transformers** for magnetically transferring AC (only) signals between rotating (green) and non-rotating parts. (a) & (b) are **flat-face** (aka **pot core**), (c) & (d) are **axial**; the stationary (black) and rotating (green) windings in (a) & (c) are **adjacent**, those in (b) & (d) are **coaxial**. Coaxial windings are more difficult to manufacture with a small **air gap** (yellow), but can be made with somewhat better magnetic coupling and thus higher efficiency. Magnetic flux lines are illustrated in red. Images are cartoon representations only; for notational clarity, the housings and bearings that keep the parts aligned and spinning freely are not shown. Note also that the individual windings of the electromagnets are usually much smaller gauge wires than suggested by the cross sections shown here.

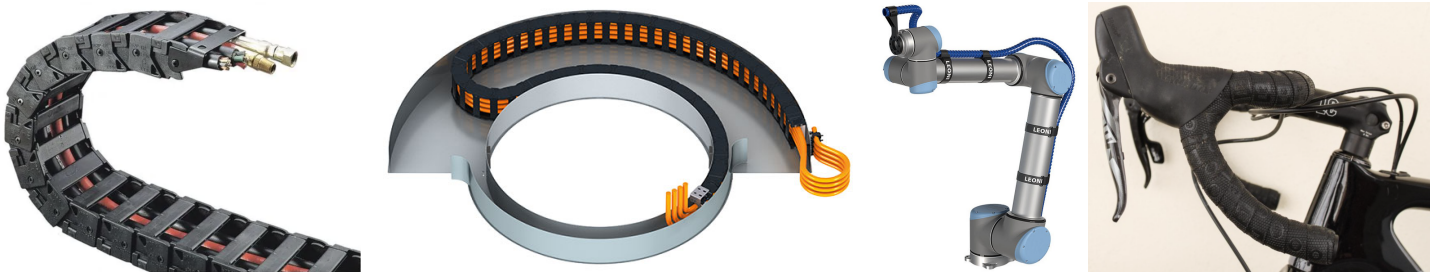

Figure 6.3: Example cable routings facilitating limited ranges of movement. (a) Linear drag chain (each link of the chain pivots in only one direction, and a finite amount, thus ensuring a prespecified minimum radius of curvature of the cables lying in the channel running through its center), (b) rotary drag chain (that is, a linear drag chain lying in a channel between two concentric walls which rotate wrt each other), and (c), (d) less-structured solutions that allow multiple degrees of freedom of movement. Cables manufactured using highly flexible silicone rubber insulation are particularly well suited for such applications.

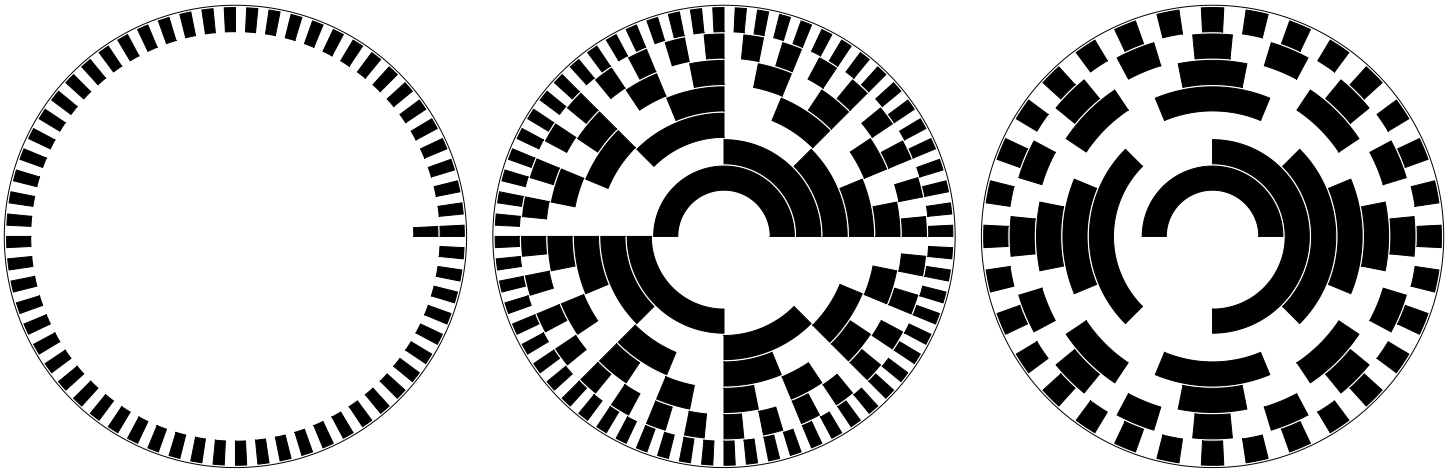

Figure 6.4: Common encoder disk slit patterns: (a) ABZ, (b) binary, (c) Gray. [Code: RR_encoders.m]

6.2 Rotary encoders and resolvers

A **rotary encoder** (often, just called an encoder) is a digital device used to measure the rotation of a shaft. Common constructions of rotary encoders are optical, mechanical, and magnetic.

An **optical** encoder consists of one or more LEDs illuminating one side of a circular **encoder disk** (mounted to the rotor shaft) with one or more rings (that is, annular rows) of slits (see Figure 6.4), and one or more photodiodes per ring of slits on the opposite side. As a slit passes in front of each photodiode, light from an LED passes through this slit, and the wire attached to that photodiode transmits a logical **pulse** (transitioning from 0 to 1, and eventually back to 0). Reflective optical encoders also exist, in which the LED(s) and the phototdiode(s) are mounted on the same side of the encoder disk.

A **mechanical** encoder energizes metal patches on a rotating disk, arranged in the same patterns as shown in Figures 6.4b or c (power is transferred to the disk using brushes and commutators; seen §6.1). Stationary brushes slide on and off these metal patches (also acting as commutators), again sending signals down the wires attached to these brushes. Due to friction and wear issues, mechanical encoders are only appropriate for shafts that are turned infrequently, and at low speed, such as the rotary selector input on a voltmeter or the volume knob on a stereo. In other applications, optical or magnetic encoders are preferred.

A **magnetic** encoder replaces the slits in a disk with magnets, and the photodiodes with magnetic (Hall effect) sensors, but otherwise again operate according to similar principles. Magnetic encoders are particularly convenient for brushless motors (see §6.9), which already have a series of permanent magnets mounted, with alternating directions of polarity, to the rotor shaft.

There are two principal types of rotary encoders, described in §6.2.1 and 6.2.2:

- **incremental**, which only count changes to the rotation angle of a shaft from its prior state, and
- **absolute**, which directly indicate the absolute phase angle of a shaft, regardless of its prior state.

Optical and magnetic encoders may be of either type; mechanical encoders are generally of the absolute type. Note that **hybrid** ABZ encoders (also discussed in §6.2.1), which are incremental over much of their range, with occasional resets at a known angle, may be considered as a third category.

A **resolver** is common analog device used to measure the rotation of a shaft, and is discussed in §6.2.3.

6.2.1 Incremental encoders (unidirectional, quadrature, and ABZ)

The simplest incremental encoder, called a **unidirectional encoder**, consists of just a single ring of slits and a single photodiode. Every time a slit passes in front of the photodiode, a pulse is generated on the wire attached

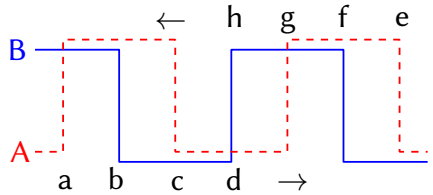

Figure 6.5: Encoder signals from a quadrature encoder, indicating the (dashed) A and (solid) B signals. These signals are generated by a pair of photodiodes placed about $90(1+4i)/n$ degrees apart (for integer i) near an encoder disk with a single ring of n slits. The $\{a, b, c, d\}$ *transitions* (from left to right in the image) indicate one direction of shaft rotation, and the $\{e, f, g, h\}$ transitions (from right to left in the image) indicate the other direction of shaft rotation. For a given n, i may be selected to make the encoder easy to manufacture (e.g., physically placing the two photodiodes around $45°$ to $90°$ apart around the shaft).

to the photodiode. A counter unit (see §1.5.5) on the MCU increments its counter in response to the rising edge, the falling edge, or both, of these pulses. This approach is only useful for shafts designed to spin in one direction, but such applications are common (in conveyer belts, assembly lines, etc.). The number of slits per revolution in the encoder disk defines the resolution of the encoder, and should be selected based on the maximum speed of rotation of the shaft and the maximum reliable rate of the counter unit. Note that motors (which often operate most efficiently at speeds much higher than needed in a particular application) often have speed-reducing (and, thus, torque-increasing) gearboxes attached. Attaching the encoder disk before (or, after) such a gearbox increases (or, decreases) the effective resolution of the encoder for a given number of slits in the encoder disk. Also, the number of slits per revolution of the encoder disk is limited by practical issues; if this number is made too high, the slits become too narrow to manufacture precisely, the state transitions of the signals from the photodiodes become noisy, and counting them becomes difficult. Thus, depending on the application specifics, mounting the encoder disk before or after the gearbox (if one is present) may be preferred.

We next consider an encoder built with a single ring of n slits, and *two* photodiodes, denoted A and B. If the two photodiodes are placed $360\,i/n$ degrees apart from each other around the shaft (for integer i), the signals that they generate will be exactly in phase with each other, and the second photodiode will provide no useful new information. If the two photodiodes are placed $180(1+2i)/n$ degrees apart from each other around the shaft, the signals that they generate will be of opposite phase, and again the second photodiode will provide no useful new information. However, if the two photodiodes are placed about $90(1+4i)/n$ degrees apart from each other around the shaft, the signals that they generate will be about $90°$ out of phase (see Figure 6.5a), which as described below is quite useful. Note that, for a given n, i may be selected to make the encoder easy to manufacture (e.g., physically placing the two photodiodes around $45°$ to $90°$ apart around the shaft).

With two signals A and B that are about $90°$ out of phase (see Figure 6.5), we can actually infer the *direction* of rotation by looking at state *transitions* (low-to-high, high-to-low, or both) of one or both logical states, while monitoring the other state, leading to a **bidirectional** incremental encoder. Transitions $\{a, b, c, d\}$, below/left, happen (only, and in this order) when time flows from left to right in Figure 6.5 (indicating, say, "clockwise" rotation), and transitions $\{e, f, g, h\}$, below/right, happen (only, and in this order) when time flows from right to left (indicating "anticlockwise" rotation):

a) A transitions from low to high when B is high,
b) B transitions from high to low when A is high,
c) A transitions from high to low when B is low,
d) B transitions from low to high when A is low,
e) A transitions from low to high when B is low,
f) B transitions from low to high when A is high,
g) A transitions from high to low when B is high,
h) B transitions from high to low when A is low.

Such a bidirectional encoder can be set up to watch for 1, 2, or all 4 of the transitions in each of the above two groups (and, to increment or decrement its counter as appropriate when these transitions are detected),

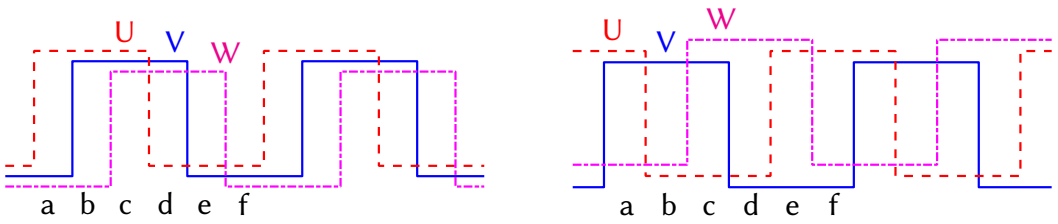

Figure 6.6: Encoder signals from (left) the $60°$ variant, and (right) the $120°$ variant, of a commutation encoder, indicating the (dashed) U, (solid) V, and (dot-dashed) W channels. These signals are picked up by a triplet of magnetic (Hall effect) sensors placed $60(1+6i)/n$ degrees apart (in the $60°$ variant), or $120(1+3i)/n$ degrees apart (in the $120°$ variant), near the n permanent magnets, of alternating polarity, mounted to the rotating shaft of a BLDC motor. The $\{a, b, c, d, e, f\}$ *phases* (note: not transitions) may be used by six-state logic driving the motor (see 6.9.1) to coordinate the application of torque on the shaft in the clockwise or anticlockwise directions. Again, for a given n, i may be selected to make the encoder easy to manufacture (e.g., physically placing the two photodiodes around $30°$ to $60°$ apart around the shaft).

referred to as **1x**, **2x**, and **4x** modes. The capability of using 4x mode (that is, of updating the counter $4n$ times per full wheel revolution) lends this sensor its common name as a **quadrature encoder**.

An **ABZ** encoder combines a (bidirectional) quadrature encoder as described above with a third photodiode mounted to detect the passage of a single narrow slit on a second ring in the encoder disk, as shown in Figure 6.4a. This third signal gives an absolute reference point on the shaft angle during each full rotation, and can be useful to initialize an absolute reference angle when restarting the system, and to correct for possible missed encoder counts during normal operation. The ABZ encoder is thus actually a hybrid between incremental and absolute encoder designs.

6.2.2 Absolute encoders (commutation, binary, and Gray)

We next consider an encoder built with n pairs of N-S poles mounted (with alternating polarity) to a rotating shaft, and *three* stationary magnetic (Hall effect) sensors, denoted $\{U, V, W\}$, mounted nearby. As illustrated in Figure 6.6, there are two distinct variants on this idea:

- if the sensors are placed about $60(1+6i)/n$ degrees apart from each other around the shaft, for integer i, the signals they generate will be about $60°$ out of phase, and
- if the sensors are placed about $120(1+3i)/n$ degrees apart from each other around the shaft, for integer i, the signals they generate will be about $120°$ out of phase.

Either way, six valid phases of rotation can be uniquely detected[3], denoted $\{a, b, c, d, e, f\}$. The inputs to the three sets of electromagnets of a three=phase BLDC motor (see §6.9) may then be synchronized to these six phases by the commutation logic (see §6.9.1) driving these sets of electromagnets in order to coordinate the motor's efficient application of torque on the shaft in the clockwise and anticlockwise directions. As a result of its utility in the commutation of BLDC motors, such an encoder is commonly called a **commutation encoder**. Note that, since a commutation encoder indicates which of six phases of rotation that a motor shaft is in, without reference to where the shaft was previously, it is referred to as an absolute encoder.

In order determine with higher resolution the absolute rotation angle of a shaft, consider again the use of an optical encoder, but now with an encoder disk with multiple rings, and a radially-aligned row of photodiodes to read the binary values (slits) in each ring. With 7 rows of slits, it is straightforward to see that $2^7 = 128$ distinct positions can be read off directly; conveniently, the sensed signal will immediately be in simple binary

[3]The states 101 and 010 are not valid in the $60°$ variant, and the states 111 and 000 are not valid in the $120°$ variant.

Gray	00000	00001	00011	00010	00110	00111	00101	00100	01100	01101	01111	01110	01010	01011	01001	01000	11000	11001	11011	11010	11110	11111	11101	11100	10100	10101	10111	10110	10010	10011	10001	10000
binary	00000	00001	00010	00011	00100	00101	00110	00111	01000	01001	01010	01011	01100	01101	01110	01111	10000	10001	10010	10011	10100	10101	10110	10111	11000	11001	11010	11011	11100	11101	11110	11111

Table 6.1: The numbers 0 to $2^5 - 1 = 31$, in binary and Gray code. [Codes: RR_bin2gray.m, RR_gray2bin.m]

order if a binary encoder pattern, such as that illustrated in Figure 6.4b, is used.

However, there is a significant problem with the above approach. Due to manufacturing inaccuracies (specifically, minor misalignments in the row of photodiodes), during the transition from a single binary number to another (say, between the state 1111111 and the state 0000000) as the encoder the encoder disk turns, some bits will inevitably change slightly before the others, making the rotation of the shaft appear, for a moment or two, to be in a vastly different state than it actually is. These errors can be quite problematical. Note further that the misalignment of the photodiodes can become significantly more severe in a system as it ages, and inevitably receives a few substantial bumps and knocks. As a result, *binary encoders should never actually be used*; there is in fact a much better approach, described next.

Consider first the following reversible transformation: start from an n-bit binary number $b(1)\,b(2)\,\ldots b(n)$, where $b(1)$ denotes the most significant bit (msb) and $b(n)$ denotes the least significant bit (lsb), and define another n-bit binary sequence $g(1)\,g(2)\,\ldots g(n)$, dubbed a **Gray code**, as follows:

$$g(1) = b(1), \quad \text{for} \quad i = 1 : n-1, \quad g(i+1) = b(i) \text{ xor } b(i+1), \quad \text{end} \tag{6.1a}$$

where xor denotes exclusive or[4]. The inverse of this operation, it is easy to prove[5], is given by

$$\bar{b}(1) = g(1), \quad \text{for} \quad i = 1 : n-1, \quad \bar{b}(i+1) = \bar{b}(i) \text{ xor } g(i+1), \quad \text{end} \tag{6.1b}$$

The transformation of the first $2^5 = 32$ binary numbers (starting from 0) to Gray code and back, by the above reversible transformations, is listed in Figure 6.1. Reading an n-bit Gray code sequence with an optical encoder, rather than reading an n-bit binary sequence, completely eliminates the problem mentioned in the previous paragraph, of some bits changing slightly before other bits when the photodiodes are slightly out of whack. This is a result of the remarkable fact that *only one bit changes at a time when counting through the numbers 0 to $2^n - 1$, and looping back to 0, when the numbers are represented using an n-bit Gray code*, as illustrated for the $n = 5$ case in Table 6.1. Further, the conversion from Gray code to a corresponding binary representation can be done remarkably quickly using the above algorithm.

Finally, one added benefit of a Gray code encoder is that, even though n bits are still needed to represent all numbers from 0 to $2^n - 1$, the *changes in the lsb happens at half the rate* as the changes in the lsb of the corresponding binary sequence (again, see Table 6.1). As mentioned previously, if the slits become too narrow to manufacture precisely, the transitions of the signals from the photodiodes become noisy, and, practically,

[4]The operation a xor b is equal to 1 (true) if its arguments differ, and is equal to 0 (false) if they are the same.

[5]That is, the reconstructed $\bar{b}(i)$ in (6.1) equals the original $b(i)$ for all i. This may be established with a **proof by induction**: assume, for some i, that $\bar{b}(i) = b(i)$. To show that it follows, for this i, that $\bar{b}(i+1) = b(i+1)$, consider the four possible cases:

(a) If $b(i) = 0$ and $b(i+1) = 0$, then $g(i+1) = b(i)$ xor $b(i+1) = 0$, and $\bar{b}(i+1) = \bar{b}(i)$ xor $g(i+1) = 0$.
(b) If $b(i) = 0$ and $b(i+1) = 1$, then $g(i+1) = b(i)$ xor $b(i+1) = 1$, and $\bar{b}(i+1) = \bar{b}(i)$ xor $g(i+1) = 1$.
(c) If $b(i) = 1$ and $b(i+1) = 0$, then $g(i+1) = b(i)$ xor $b(i+1) = 1$, and $\bar{b}(i+1) = \bar{b}(i)$ xor $g(i+1) = 0$.
(d) If $b(i) = 1$ and $b(i+1) = 1$, then $g(i+1) = b(i)$ xor $b(i+1) = 0$, and $\bar{b}(i+1) = \bar{b}(i)$ xor $g(i+1) = 1$.

In all four cases, $\bar{b}(i+1) = b(i+1)$; i.e., (6.1b) inverts the transformation done by (6.1a). This applies identically for the "base case" $i = 1$ [$b(1) = g(1) = \bar{b}(1)$], and thus, successively, for the case with $i = 2$, and then for $i = 3$, etc., ultimately for all integer $i \geq 1$.

sensing them becomes difficult. The severity of this problem is reduced in a Gray code encoder, as, at a given resolution n, the smallest slits are twice as wide as for the corresponding binary encoder, as readily apparent in the 7-bit Gray code encoder disk illustrated in Figure 6.4c.

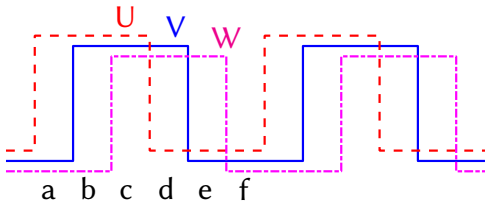

Figure 6.7: An analog resolver for determining the angle of a rotating shaft: (a) Configuration of the coils. (b) Block diagram of the circuit used, in *control transformer* mode, to process the measured signals V_s and V_c that arise due to the excitation signal $V_r = A\sin(\omega_e t)$. (c). Block diagram of the circuit used, in *control transmitter* mode, to process the measured signal V_r that arises due to the excitation signals $V_s = A\sin(\omega_e t)$ and $V_c = A\cos(\omega_e t)$.

6.2.3 Resolvers

In contrast with the encoders described previously, which are digital devices, a **resolver** is an *analog* device used to measure the rotation angle of a shaft. It is formed with two stationary coils placed $90°$ apart around the shaft, and one coil placed on the rotating shaft itself, as illustrated in Figure 6.7a. A high frequency sinusoid is use to drive either the stationary coils (in **control transmitter** mode) or the rotating coil (in **control transformer** mode); the relative phase of the induced current on the remaining coil(s) is then measured to determine the angle $\theta(t)$ of shaft at that time t (with electrical excitation frequency ω_e assumed to be much faster than the frequency of shaft rotation, $\omega_s = d\theta/dt$).

In either case, an AC signal (carried over two wires, one of which may be thought of as ground) must be transmitted to or from the rotating shaft (this is the measured signal in control transmitter mode, and the driving signal in control transformer mode). This may be done using brushes and commutators, or using a rotating transformer, as discussed in detail in §6.1.

In control transformer mode, driving the rotating coil with $V_r = A\sin(\omega_e t)$, the current induced in the stationary coils will be accompanied by voltage fluctuations $V_s = \beta A\sin(\omega_e t)\sin\theta$ and $V_c = \beta A\cos(\omega_e t)\cos\theta$. The coefficient β is related to the magnetic induction efficiency, but is ultimately unimportant

In control transmitter mode, driving the stationary coils with $V_s = A\sin(\omega_e t)$ and $V_c = \beta A\cos(\omega_e t)$, the current induced in the rotating coil will be accompanied by a voltage fluctuations $V_r = \beta A\sin(\omega_e t)\sin\theta$. The ...

6.3 Inertial Measurement Units (IMUs): accels and gyros

MEMS accels, gyros,

6.4 Magnetometers, barometers, and GNSS/GPS systems

and magnetometers

Examples of GNSS include GPS, GLONASS, Galileo, Beidou

6.5 Triangulation & trilateration

6.5.1 Beacon-based solutions

6.5.2 Motion Capture (MoCap) in controlled lab environments

Passive and active markers.

via visual & RF beacons and microphone arrays

“ground truth"’

6.6 Depth imaging

RGB-D

2D and 3D Lidar

Example: Big box store

Camera-based systems

Optical flow and visual SLAM (Simultaneous Localization and Mapping)

Broadband high-frequency RF MoCap

3-10 GHz

IndoTraq

6.7 Other sensors

6.7.1 Strain gauges

Piezoelectric effect

6.7.2 Liquid level sensors and flow meters

6.7.3 Thermocouples and Ph meters

6.8 Brushed DC (BDC) Motors and Steppers

To model (in SI units; see §10.1.1-10.1.2) the dynamics of a brushed DC (BDC) motor, we first consider the following functions of time

- $V(t)$ is the **voltage** applied to the motor [averaged over each PWM cycle, and measured in volts],
- $I(t)$ is the **current** through the motor [measured in amps],
- $\omega(t)$ is the **rate of rotation** of the motor shaft [measured in rad/s],
- $\tau(t)$ is the **torque** applied by the motor to the mechanical load [measured in N·m],

A representative high-fidelity model of the voltage and torque balances, respectively, of a BDC motor is then given by

$$V = RI + L\,dI/dt + K\omega, \tag{6.2a}$$
$$\tau = KI = J\,d\omega/dt + b\omega + C\,\mathrm{sgn}(\omega), \tag{6.2b}$$

where the last term in (6.2b) models dry friction (see Example **??**), and where

- R is the motor **resistance** [measured in ohms],
- L is the motor **inductance** [measured in henries],
- K is the **torque constant** of the motor [measured in N·m/A = V/(rad/s)],
- J is the **rotational interia** of both the motor and its load [measured in N·m/(rad/s^2)],
- b is the **viscous friction coefficient** [measured in N·m·s, and
- C is the **dry friction coefficient** [measured in N·m; see (**??**)].

Note that the torque constant K appears in both the computation of the torque generated by the motor, Ki, in (6.2b), as well as the **back emf** in the electric circuit, $K\omega$, in (6.2a). The parameters in such a model may be determined by accelerating and decelerating a flywheel of known rotational inertia mounted to the motor shaft a number of times, while monitoring the rate of rotation of the shaft with encoders, then performing a least squares fit.

A convenient lower-fidelity model of a BDC motor that is sometimes adequate for the purpose of applying feedback control is to assume that $R = L = J = 0$ in (6.2). Note that this simplified model neglects altogether the dynamics (that is, the d/dt terms) in (6.2). Given a certain operating voltage V, two data points are then measured: the torque at zero angular velocity (that is, $\{\tau, \omega\} = ??$), and the ...

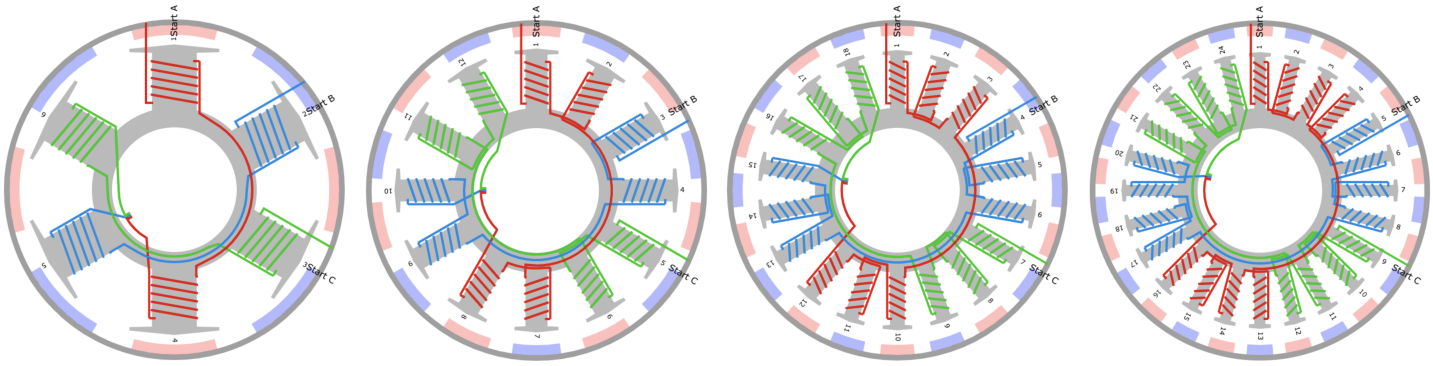

Figure 6.8: Some efficient outrunner brushless (BLDC) motor configurations (6s8p, 12s14p, 18s20p, 24s26p), shown with Wye termination. In BLDC motors, the electromagnets are stationary, and the permanent magnets rotate with the shaft. Commutation (that is, coordination of the electrical signals causing the motor to turn) is thus achieved electronically rather than mechanically. The windings of these particular three-phase motors are given by $(ABC)^2$, AabBCcaABbcC, $(AaABbBCcC)^2$, and AaAabBbBCcCcaAaABbBbcCcC (see text). Images generated via the convenient online tool available at http://www.bavaria-direct.co.za/.

6.9 Brushless DC (BLDC) Motors

A BLDC motor consists of n_s stationary[6] electromagnets, and n_p permanent magnets[7] (of alternating polarity) attached to a rotating shaft. Both sets of magnets are placed in a circular arrangement around the shaft, with a very small air gap between them. The (rotating) permanent magnets may be placed to the inside [called an **inrunner** configuration] or to the outside [called an **outrunner** configuration] of the (stationary) electromagnets. BLDC motor designs are commonly denoted n_s s n_p p; a few examples are given in Figure 6.8.

As the electromagnets are stationary in brushless (BLDC) motors, they are commutated electronically; this is in contrast with brushed (BDC) motors, in which the electromagnets rotate and the permanent magnets are stationary, and for which mechanical commutation (with brushes and split-ring commutators) is used instead (see §6.8 and §6.1). **Three-phase** commutation of the electromagnets, in which the n_s stationary electromagnets are electrically arranged into 3 equal-sized groups that are powered $120°$ out of phase from each other, are by far the most common, and form the focus of our study[8]. The algorithms used to coordinate the electronic commutation of three-phase BLDC motors with the rotation of the shaft is discussed further in §6.9.1-6.9.3.

Note that the ends of the three sets of electromagnets may be tied together in a Y (aka wye) configuration, as illustrated in Figure 6.8, or arranged in a triangular Δ (aka delta) configuration. For a given set of windings, the wye configuration has $\sqrt{3}$ times more torque per amp in each phase; if the motor is rewound (with more turns of thinner wire), the performance of the delta configuration can be made to be roughly equivalent.

The number of "slots" n_s (a multiple of 3), and the number of "poles" n_p (a multiple of 2) are important parameters in a BLDC motor design[9]. To make maximum use of the volume that the motor occupies for torque production, these two numbers should be close to the same, but not equal. If $n_s = n_p$, then at certain rota-

[6] The maximum number of electromagnets may be determined by counting the **slots** through which the wires are threaded when winding the electromagnets; n_s is thus often said to indicate the number of slots through which these wires are thread.

[7] Rare earth magnets made from Neodymium (Nd) or Samarium Cobalt (SmCo) are most commonly used in BLDC motors.

[8] Note that five-phase (and, even, seven-phase and nine-phase) BLDC motor designs are also possible, with improved efficiency and fault tolerance, but with substantially more complex coordination circuitry.

[9] We focus the present discussion on the case in which every adjacent pair of "slots" is used to wrap a coil, thus making an electromagnet out of the (iron-core) post in between each pair of slots (see Figure 6.8). This is sometimes said to be a "two-layer" configuration in which, looking down in any individual slot, two coils are visible: those going around the post on one side, and those going around the post on the other. This is in contrast to the "one-layer" configurations sometimes encountered, in which, looking down in any individual slot, only one coil is visible, with alternating posts not coiled to form electromagnets.

tion angles all the electromagnets and permanent magnets are aligned, and the motor can not self start; this configuration should thus be avoided.

For a given n_s and n_p for a three-phase motor, the following characteristics are commonly defined:

$$\text{slot/pole ratio:} \qquad q = n_s/(3n_p), \tag{6.3a}$$

$$\text{pole units:} \qquad u = \gcd(n_s, n_p), \tag{6.3b}$$

$$\text{coils per phase per pole unit:} \qquad z = n_s/(3u) \quad \Leftrightarrow \quad 3\,u\,z = n_s, \tag{6.3c}$$

$$\text{cogging steps:} \qquad c = \text{lcm}(n_s, n_p), \tag{6.3d}$$

where gcd denotes the greatest common divisor, and lcm denotes the least common multiple.

To keep n_s close to but not equal to n_p for efficient use of the motor volume, as suggested previously, a **slot/pole ratio** in the range $0.25 \leq q \leq 0.5$ is generally advised.

The number of **pole units** u is the maximum number of electromagnets that align with a permanent magnet at any moment. The loading on the motor is said to be **symmetric** when $u > 1$; configurations that are not symmetric should be avoided, as the torque produced by the electromagnets would cause the motor to wobble. The quantity z measures the number of **coils per phase per pole unit**. The windings are **balanced** when z is an integer; configurations which are not balanced should also be avoided. The values of u and z for several recommended $\{n_s,\, n_p\}$ combinations is given in Table 6.2, directly eliminating from consideration: (a) those with $n_s = n_p$, (b) those regions outside the recommended slot/pole ratio range of $0.25 \leq q \leq 0.5$, (c) those without symmetry, and (d) those that are out of balance. Also listed in Table 6.2 is the electrical excitation frequency $f_e = f_s n_p/2$ associated with shaft rotation at $f_s = 100\,\text{Hz} = 6000\,\text{rpm}$.

To illustrate, the four designs in Figure 6.8 each have $u = 2$ pole units (and are thus symmetric), and the values of z for these four designs are 1, 2, 3, and 4 respectively (and each are, thus, balanced).

The quantity c counts the number of times that permanent magnets align directly with electromagnets during an entire revolution of the shaft (as mentioned previously, u permanent magnets simultaneously align with electromagnets each time this happens). This quantity also indicates the number of times that the torque of the BLDC reaches a minimum (and, a maximum) during one complete revolution of the shaft, dubbed the **cogging steps** of the motor. The larger c is, the smaller the amplitude of this **torque ripple**. The worst torque ripple is given for an equal number of slots and poles, for which $c = n_s = n_p$, again suggesting that this condition should be avoided. Values of c for several recommended $\{n_s,\, n_p\}$ combinations is given in Table 6.3.

We next consider how the individual electromagnets of a brushless motor should be wound. Denote the three electrical phases driving the BLDC motor as $\{\text{A}, \text{B}, \text{C}\}$, and let $\{\text{A}, \text{a}, \text{B}, \text{b}, \text{C}, \text{c}\}$ denote windings of these phases, where uppercase denotes clockwise (CW) windings, and lowercase denotes anticlockwise (ACW) windings. A BLDC motor configuration with 6 clockwise windings (with $u = 2$ and $z = 1$) may thus be denoted ABCABC, or more compactly as $(\text{ABC})^2$. Defining the (dLRK) winding as AabBCcaABbcC, and also defining

(i) as ABbcaABCcabBCAabcC,
(ii) as $(\text{AaABbBCcC})^2$,
(iii) as $(\text{AabBCcaABbcC})^2$ = $(\text{dLRK})^2$,
(iv) as AaAabBbBCcCcaAaABbBbcCcC,
(v) as $(\text{AaABbBCcC})^2$,
(vi) as ABCcabcaABCABbcabcCABCAabcabBC,
(vii) as AaABbcCcaABbBCcaAabBCcCAabBbcC,
(viii) as $(\text{AaAaABbBbBCcCcC})^2$,

recommended winding patterns that maximize the torque output for several recommended $\{n_s,\, n_p\}$ combinations are given in Table 6.4. Note in particular that, for those $\{n_s, n_p\}$ combination with $z = 1$, the symmetric answer must simply be $(\text{ABC})^u$, by inspection. Further, $(\text{ACB})^u$ is just $(\text{ABC})^u$ operating in reverse.

The remaining winding patterns listed above may be motivated fairly simply via symmetry arguments on a case-by-case basis, and are not nearly as mysterious as they might at first look. For example, consider first the 24s26p design, rotated just a couple of degrees from the configuration shown at right in Figure 6.8, such that there is (pink) permanent magnet exactly halfway between the (CW-wound) electromagnet 7, and the

$n_s \downarrow$ \ $n_p \rightarrow$	4	6	8	10	12	14	16	18	20	22	24	26	28	30	32	34
6	2, 1		**2, 1**													
9		3, 1			3, 1											
12			4, 1	2, 2		**2, 2**	4, 1						$q<0.25$			
15				5, 1					5, 1							
18					6, 1	2, 3	2, 3		**2, 3**	2, 3	6, 1					
21						7, 1							7, 1			
24							8, 1		4, 2	2, 4		**2, 4**	4, 2		8, 1	
27								9, 1			3			3		
30		$q>0.5$							10, 1	5		2, 5	2, 5		**2, 5**	2, 5
33										11, 1						
36											12, 1	2, 6	4, 3	6, 2	4, 3	2, 6
f_e	200	300	400	500	600	700	800	900	1000	1100	1200	1300	1400	1500	1600	1700

Table 6.2: Pole units and coils per phase per pole unit, $\{u,\ z\}$, of 3-phase motors with recommended combinations of [left] the number of slots n_s and [top] the number of poles n_p. Non-recommended regions include:
those with $n_s = n_p$, which are not self starting, and have relatively poor cogging numbers,
those with a slot/pole ratio $q = n_s/(3n_p)$ outside the range $0.25 \leq q \leq 0.5$, which are inefficient,
those without symmetry, which wobble, and
those that are electrically out of balance, with more windings on some phases than others.
Also listed is the electrical excitation frequency f_e associated with shaft rotation at $f_s = 100\,\text{Hz} = 6000\,\text{rpm}$.
Code to generate and extend Tables 6.2, 6.3, 6.5: RR_BLDC_design.m.

$n_s \downarrow$ \ $n_p \rightarrow$	4	6	8	10	12	14	16	18	20	22	24	26	28	30	32	34
6	12		**24**													
9		18			36											
12			24	60		**84**	48									
15				30					60							
18					36	126	144		**180**	198	72					
21						42							84			
24							48		120	264		**312**	168		96	
27								54			216			270		
30									60	330		390	420		**480**	510
33										66						
36											72	468	252	180	288	612

Table 6.3: Cogging steps c (larger is smoother) of 3-phase motors for recommended $\{n_s,\ n_p\}$ combinations.

$n_s \downarrow$ \ $n_p \rightarrow$	4	6	8	10	12	14	16	18	20	22	24	26	28
6	$(ABC)^2$		$(ABC)^2$										
9		$(ABC)^3$			$(ABC)^3$								
12			$(ABC)^4$	(dLRK)		(dLRK)	$(ABC)^4$						
15				$(ABC)^5$							$(ABC)^5$		
18					$(ABC)^6$	(i)	(ii)			(ii)	(i)	$(ABC)^6$	
21						$(ABC)^7$							$(ABC)^7$
24							$(ABC)^8$			(iii)	(iv)	(iv)	(iii)
27								$(ABC)^9$			(v)		
30									$(ABC)^{10}$	(vi)		(vii)	(viii)

Table 6.4: Recommended winding configurations of 3-phase motors for recommended $\{n_s,\ n_p\}$ combinations. $(ABC)^2$ denotes ABCABC, etc., where {A,B,C,a,b,c} denote (uppercase) CW and (lowercase) ACW winds of phases A, B, and C. Winding (dLRK) denotes AabBCcaABbcC; windings (i) through (viii) defined in the text.

$n_p \rightarrow$ / $n_s \searrow$	4	6	8	10	12	14	16	18	20	22	24	26	28	30	32	34
6	0.866		**0.866**													
9		0.866			0.866											
12			0.866	0.933		**0.933**	0.866									
15				0.866					0.866							
18					0.866	0.902	0.945		**0.945**	0.902	0.866					
21						0.866							0.866			
24							0.866		0.933	0.949		**0.949**	0.933		0.866	
27								0.866			0.945			0.945		
30									0.866	0.874		0.936	0.951		**0.951**	0.936
33										0.866						
36											0.866	0.867	0.902	0.933	0.945	0.953

Table 6.5: Fundamental winding factor k_{w1} (larger is more powerful) for recommended n_s and n_p combinations.

(ACW-wound) electromagnet 6. If the B phase is sinusoidal, and is phased such that the magnetic field at electromagnets 6 and 7 (which are of opposite polarity) peak at this moment, then a maximum force will be exerted on the (pink) permanent magnet halfway in between (ditto on the blue permanent magnet on the opposite side). Looking around the circumference at the other permanent magnets that, at this instant, are closest to being halfway between two electromagnets suggests that the electromagnet pairs {5,6} and {7,8} should also peak at roughly the same time (and, again, be of opposite handedness); again, ditto on the opposite side. By symmetry, this suggests that, for the 24s26p design, the $z = 4$ electromagnets of each phase, in each of the $u = 2$ pole units, should be placed next to each other, and with opposite handedness. The handedness at the intersections between the different sets of phases in each pole unit (that is, ab, BC, ca, AB, bc, CA) is then selected in the sense that continues to apply torque in the same direction, finally arriving at winding (iv). The other winding patterns listed above (and, those for larger $\{n_s, n_p\}$ configurations) may be reasoned similarly.

A more detailed discussion of the electromagnetic forces within a BLDC motor is beyond the scope of the present discussion. A definitive text on this subject is Hendershot & Miller (2010); we will simply state here the primary definitions that arise in this analysis, leaving derivation and detailed discussion to this text:

$$\text{slot-pitch angle:} \qquad \gamma_s = \pi n_p / n_s = \pi/(3q), \tag{6.4a}$$

$$\text{coil-span angle:} \qquad \epsilon = \pi - \gamma_s, \tag{6.4b}$$

$$\text{pitch factor, aka coil-span factor:} \qquad k_{pn} = \cos(n\epsilon/2), \tag{6.4c}$$

$$\text{distribution factor:} \qquad k_{dn} = \sin(n\sigma/2)/[z\sin(n\sigma/(2z))] \quad \text{where} \quad \sigma = \pi/3, \tag{6.4d}$$

$$\text{winding factor:} \qquad k_{wn} = k_{dn} k_{pn}. \tag{6.4e}$$

As discussed in the above-mentioned text, the **fundamental winding factor** k_{w1} (that is, k_{wn} with $n = 1$), as defined by (6.3)-(6.4), is proportional to the total torque that a BLDC motor can generate. Generally, the higher k_{w1} is the better; note that $0.866 \leq k_{w1} < 1$ for the recommended BLDC motor designs listed in Table 6.5.

In summary, all of the configurations listed in Tables 6.2-6.5 are viable three-phase BLDC designs, and may be reached by the motor designer for different applications, depending on the relative importance placed on:

- simplicity of construction, for which small n_s and small n_p are preferred,
- efficiency, for which a large fundamental winding factor k_{w1} is preferred, and
- smoothness of operation, for which a large number of cogging steps c is preferred.

As highlighted in Tables 6.2-6.5, some particularly good tradeoffs between simplicity of construction, efficiency, and smoothness of operation include the **6s8p**, **12s14p**, **18s20p**, **24s26p**, and **30s32p** designs, with windings of $(ABC)^2$, (dLRK), (ii), (iv), and (viii), respectively, as defined above (see Figure 6.8).

6.9.1 Trapezoidal (“six-state”) commutation

simple

6.9.2 Sinusoidal commutation

minimizes torque ripple

6.9.3 Field oriented control

Third harmonic, higher torque.

6.10 Induction Motors

6.11 Servos and Electronic Speed Controllers (ESCs)

blah.

6.12 Other actuators

6.12.1 Linear actuators and solonoids

6.12.2 Hydraulic and pneumatic actuators

6.12.3 Artificial muscle and electroactive polymers

6.13 Light Emitting Diodes (LEDs), buttons, and Charlieplexing

6.13.1 Debouncing

6.14 Displays and other interfaces

6.14.1 TFT, LCD, OLED

6.14.2 Capacitive or resistive touch screens

6.14.3 eInk

6.14.4 Persistance of Vision (POV)

...

Part II

Theoretical Foundations